(2) 改変型 tissue-plasminogen activator(t-PA)

・Reteplase(Retavase®)

t-PAのドメインのうち，K2ドメイン(Kringle2ドメイン)とPドメイン(プロテアーゼドメイン)の2つのドメインのみからなる改変体。非改変型のt-PAでは血中半減期が約3分であるため，点滴静注(持続投与)によりようやく薬効が得られるが，Reteplaseの血中半減期は90分以上と延長されており，単回の静脈内投与が可能となっている。また，フィブリン親和性減少のため，血栓への浸透性が高く，血栓の速やかな溶解が可能であるとされている。

・Tenecteplase(TNKase®)

t-PAのK1ドメインの103番目のThrをAsnに，117番目のAsnをGluに置換し，Pドメインの4つのAlaを置換した改変体。非改変型と比較して，フィブリン親和性および，t-PAの阻害因子であるplasminogen activator inhibitor-1への抵抗性が上昇し，血中半減期が延長されている。

・Pamiteplase パミテプラーゼ(ソリナーゼ®)

t-PAのK1ドメインを欠損させ，天然型t-PAでN末端から275番目のArgをGluに置換した改変体。フィブリンに対する高い親和性を有し，プラスミノーゲン活性化作用がフィブリンにより顕著に増強され，血中半減期も延長されている。

(3) 改変型インターフェロン

・Interferon alfacon-1

インターフェロン アルファコン-1(アドバフェロン®)

ヒトインターフェロンアルファの12種類のサブタイプのアミノ酸配列において，各位置のアミノ酸を出現頻度の最も高いアミノ酸に置換した改変体。コンセンサスインターフェロンとも呼ばれる。現在臨床に供されている「PEG非修飾型」のインターフェロンアルファ(主としてインターフェロンα2a/α2b)と比較して，高い抗ウイルス活性，抗肝炎活性を示す。

(4) 改変型顆粒球コロニー刺激因子

・Nartograstim ナルトグラスチム(ノイアップ®)

Granulocyte colony stimulating factor(G-CSF)のN末端側から1，3，4，5，17番目のアミノ酸がAla，Thr，Tyr，Arg，Serに置換した改変体。天然型のG-CSFと比較して，約3倍の比活性を示す。

2.2 糖鎖改変型

(1) 糖鎖改変型グルコセレブロシダーゼ

・Imiglucerase イミグルセラーゼ(セレザイム®)

CHO細胞で生産されたβ-グルコセレブロシダーゼをシアリダーゼ，β-ガラクトシダーゼおよびヘキソサミニダーゼの酵素処理により糖鎖末端をマンノースにした改変体。標的細胞であるマクロファージ表面に存在するマンノース受容体を介して細胞に取り込まれる。レセプターへの標的指向能，レセプター介在性のエンドサイトーシス能を有するDDS製剤と位置づけられる。

(2) 糖鎖改変型エリスロポエチン

・Darbepoetin alfa ダルベポエチン アルファ(ネスプ®)

5ヵ所のアミノ酸置換により，天然のerythropoietin(EPO)にN型糖鎖結合部位を新たに2ヵ所導入した改変体。天然のEPOには3本のN結合型糖鎖と1本のO結合型糖鎖が付加されているが，ダルベポエチンアルファでは，5本のN結合型糖鎖と1本のO結合型糖鎖が結合している。結合糖鎖が増えることにより血中半減期が延長され，投与量・投与回数の削減が期待される。

2.3 PEG結合型

(1) PEG結合型インターフェロン

・Peginterferon alfa-2a

ペグインターフェロン アルファ-2a(ペガシス®)

インターフェロンアルファ-2aのリジン残基(主な部位：第31位，第121位，第131位，第

134位)の1ヵ所に，1分子の分枝ポリエチレングリコール(分子量：約40,000)が，アミド結合を介して共有結合している修飾タンパク質(分子量：約60,000)。血中半減期が従来の約10倍に延長されており，投与量・投与回数の削減，抗原性の低下が期待される。そのため，患者のコンプライアンスの向上に大きく貢献している。

・Peginterferon alfa-2b

ペグインターフェロン アルファ-2b

(ペグイントロン®)

インターフェロンアルファ-2bのアミノ酸残基(Cys^{1}, His^{7}, Lys^{31}, His^{34}, Lys^{49}, Lys^{83}, Lys^{112}, Lys^{121}, Tyr^{129}, Lys^{131}, Lys^{133}, Lys^{134}, Ser^{163}およびLys^{164})の1ヵ所に1分子のメトキシポリエチレングリコール(平均分子量：約12,000)がカルボニル基を介して共有結合している修飾タンパク質(分子量：約32,000)。血中半減期が延長されており，投与量・投与回数の削減，抗原性の低下が期待される。

(2) PEG結合型顆粒球コロニー刺激因子

・Pegfilgrastim(Neulasta®)

大腸菌で生産されたG-CSF(フィルグラスチム)のN末端アミノ酸に，メトキシポリエチレングリコールプロピオンアルデヒド(平均分子量：約20,000)を1分子結合させた修飾タンパク質。血中半減期が延長されており，投与量・投与回数の削減が期待される。

(3) PEG結合型成長ホルモン誘導体

・Pegvisomant ペグビソマント(ソマバート®)

Human growth hormone(hGH)のアミノ酸配列を9ヵ所置換することにより，hGH受容体アンタゴニストとして作用するよう改変したタンパク質にPEG化を施した修飾タンパク質。タンパク質1分子あたり，4～6分子のPEG(分子量5,000)がLys残基に結合しており，体内安定性や血中滞留性の向上が期待される。

2.4 融合タンパク質

・Denileukin Diftitox(Ontak®)

Diphtheria toxinの一部(Met1～Thr387)-HisとInterleukin 2(IL-2)の一部(Aln1～Thr133)からなる融合タンパク質。リンパ腫細胞表面のIL-2受容体に結合し，受容体リガンド複合体として細胞内に取り込まれる。IL-2受容体の発現細胞へのターゲティング能を有し，これらの細胞特異的にジフテリアトキシンによるタンパク質合成阻害に基づいた細胞死を誘導する。

・Etanercept エタネルセプト(エンブレル®)

ヒトTumor necrosis factor(TNF)受容体p75の細胞外のリガンド結合ドメインとヒトIgGのFc部分の融合タンパク質。細胞表面のTNF受容体へのTNFの結合を拮抗的に阻害する。Fc部分は血中半減期延長や可溶型受容体の二量化(リガンド【TNF】への親和性向上)の役割を持つ。

・Alefacept(Amevive®)

ヒトluekocyte function antigen 3(LFA-3)の細胞外領域であるCD2結合ドメインとヒトIgG1のFcドメインの融合タンパク質。CD2抗原を表面に発現しているTリンパ球に選択的に結合し，リンパ球の活性化を阻害する。

・Abatacept(Orencia®)

ヒトCTLA-4の細胞外ドメインとIgG1のFcドメインの融合タンパク質。抗原提示細胞(APC)上に存在するCD80/CD86分子に結合することにより，CD28分子を介したT細胞の活性化が阻害される。

3. 新たな機能性人工タンパク質の創出技術

従来から多くのバイオ研究機関が，特定レセプターへの親和性や選択性に優れた“生理活性タンパク質のアミノ酸置換体(機能性人工タンパク質)”を創製するため，Kunkel法などの点突然変異法を用いた構造変異体(アミノ酸置換体)の作製を精力的に試みている。しかし点突然変異法は，1つ1つのアミノ酸を置換した変異体を作製し，個々の変異体を別々に精製し機能評価しなければならないため，莫大な時間と労力を要するうえ，評価できる変異体の数には実質的に限界があり，有効な変異体の効率的・効果的な作製とはいえなかった。それに対して近年，ファージ表面提示法を利用することにより10^8種類以上もの多様性を有した構造変異タンパク質(生理活性タンパク質のアミノ酸置換体)を一挙にCombinatorial Biosynthesisし，この構造変異体ライブラリーの中から，レセプター親和性や特異性などが向上した“機能性人工タンパク質”を迅速かつ効率よくスクリーニングできる基盤技術が開発されている。

ファージ表面提示法を用いたスクリーニングでは，ファージ表面にタンパク質を発現させ，固定化された標的分子と結合するファージを選別する操作を繰り返して，目的の結合特性を示すタンパク質を発現するファージを選択していく。また，選択されたファージを大腸菌に感染させれば，その培養上清中にタンパク質を発現させ，これを用いて，タンパク質の生物活性もハイスループットに評価することが可能である。さらに，培養上清というクルードなサンプルでは必ずしも評価できない発現タンパク質の物理化学的性質や生物学的性質を詳細に解析する必要がある場合には，発現させた変異体タンパク質を精製して評価を行うこともできる。

多数の変異体を評価できるという利点を活かし，ファージ表面提示法を用いて，従来の方法では見出すことのできなかった構造変異体の探索に成功した例として，腫瘍壊死因子(TNF)のリジン欠損体が報告されている[2)]。従来の点突然変異法を用いた構造－活性相関研究では，TNFのLys11やLys65・Lys90はその立体構造(三量体)形成やレセプター結合に必須と報告されていた。TNFに限らず，一般にリジン残基は多くの場合，生理活性タンパク質の高次構造形成やリガンドーレセプター結合などに必須の役割を担っているため，他のアミノ酸への置換は致命的な活性低下を招いてしまうことが，従来までの点突然変異解析によって常識となっていた。しかしファージ表面提示法を用いることで，Lys11やLys65・Lys90を含む全6個のリジン残基を一挙に他の様々なアミノ酸へ置換したタンパク質ライブラリーを構築することが可能となった結果，野生型TNFと同等さらには10倍以上もの生物活性を有するリジン欠損TNFを創製できることが判明した[2)]。この例では，TNFの6ヵ所のリジン残基を他の各種のアミノ酸に置換したTNF変異体ライブラリーをファージに導入し，固定化したTNF受容体への結合能を有するTNF変異体を発現しているファージをBiacore®を用いて選別，さらに，選別されたファージを感染させた大腸菌の上清を用いたバイオアッセイ(TNF感受性細胞に対する細胞傷害性試験)により，変異体の生物活性を評価している。リジン残基を置換しても活性を保持した変異体が得られた理由としては，リジンから置換されたアミノ酸が，TNFの活性保持に適したアミノ酸であったことが考えられる。従来の点突然変異法を用いた検討では，リジンをアラニンなどのアミノ酸に置換してTNFの活性が失われることを評価しているが，6ヵ所あるリジン残基をリジン以外のアミノ酸19種類に置換した変異体(19^6種類)の機能を個別に評価することは現実的でないこともあり，活性を保持したリジン欠損体を見出す試みはなされていなかった。ファージ表面提示法を駆

使することにより現在までに，TNF 受容体サブタイプに選択的に結合する機能性人工 TNF や，体内安定性に優れた機能性人工TNFも多数得られており[3]，今後の研究の進捗に期待が持たれるところである。

このようなファージ表面提示法を利用した機能性人工タンパク質の創出以外にも，ジーン・シャッフリング法や種々糖鎖修飾テクノロジーの開発が広く進められており，今後の“有効かつ安全なタンパク質性医薬品候補”の分子設計に寄与するものと考えられる。

4. 機能性人工タンパク質の品質・安全性確保

タンパク質性医薬品において薬効を期待される作用機構の代表的なものは，生体の恒常性維持機構の中で，本来，時空間的に厳密な発現制御のもとで発現・機能すべきであった当該タンパク質が欠損あるいは質的，量的に変化していることが発症の原因であった場合，あるいは疾患状態で質的，量的に変化したり欠損していくような場合に，これを補うというものである。そのような使用目的で開発されてきたものとしては，ヒトインスリン，グルカゴン，成長ホルモン，インスリン様成長因子，ナトリウム利尿ペプチド，グリコセレブロシダーゼ，エリスロポエチン，顆粒球コロニー刺激因子，血液凝固因子類などが典型的な例として挙げられる。その作用プロファイルがすでにほぼ明らかにされている天然型タンパク質と同等のものとして製造されたタンパク質性医薬品では，必要とされる品質が確保され，投与後の生体内濃度や作用局所さえ適正に制御できれば，一定の安全性を確保できるものと期待される。これに対して，天然のものとは異なる構造を持つ機能性人工タンパク質の品質および安全性の確保のためには，従来までのタンパク質性医薬品で必要とされていた品質・安全性確保のための方策に加え，機能性人工タンパク質の特性に応じた個別の配慮が必要になる。

タンパク質性医薬品の品質・安全性等を確保するためには，まず申請しようとする製造方法を明らかにする必要がある。そして得られた原薬について，その構造・組成，物理化学的性質，免疫化学的性質，生物学的性質などの分子特性や安定性を最新の解析法を用いて詳細に解析するとともに，目的物質関連物質や目的物質由来不純物（定義については第3章概論および ICH Q6B 参照），製造工程由来不純物などの存在状況，感染性物質が存在しないこと，その他の汚染物質の存在実態等を含めた「品質特性」（定義については ICH Q5E を参照）を明らかにすることが必要である。また，製剤の製造方法と「品質特性」についても必要な情報やデータを明らかにする必要がある。その上で，臨床の場に，適切な品質を有する医薬品を恒常的に提供するための品質確保，品質管理の方策を講ずる必要がある。品質確保，管理のキーポイントは非臨床および臨床試験により有効性，安全性が評価された製品の「品質特性」をいかに継続して保証するかということである。その際，製品レベルでのロットごとの試験による保証（適切な規格・試験法の設定）と製造方法での保証（原材料や添加物などの品質管理，重要工程の一定性，プロセス評価・検証，プロセスコントロール・工程内管理試験など）を相互補完的にいかに合理的に組み合わせて品質確保策とするかが最大の課題となる。なお開発段階においては，非臨床および臨床試験により明らかになる有効性・安全性の解析結果と品質との関連を評価・検討し，望ましい品質を確保できるよう製造方法を最適化したり，品質の一定性を確保するための規格・試験法の改定を図ったりすることが必要な場合もある。試験法には，特性解析に用いた分析手法を適切に応用する。製品の安全性評価を行う際には，その「品質特性」から考えられる安全性上の懸念事項につ

いて，特に注意して解析を行う必要があるが，機能性人工タンパク質の場合は，化学修飾により製造される修飾タンパク質の修飾位置異性体の問題，構造改変により目的以外の生物活性が変化している可能性，抗原性の問題，などが特に留意すべきポイントである。

製造工程でPEG化，デキストランやマンノース等を用いた糖修飾のような化学的改変(化学修飾)を行う場合，人為的に施されるPEG化反応や糖付加反応などはタンパク質の部位特異的に起こるものではないため，1種類あるいは数種類のアミノ酸に，しかも複数ヵ所にPEGあるいは糖などがランダムに導入される場合が多い。したがって，PEG化反応あるいは糖修飾後の機能性人工タンパク質はPEG化あるいは糖修飾された部位，導入されたPEGや糖の分子数などにおいて異なる構造を持つ分子種の混合物となり，分子量などを指標に精製された画分についても，修飾位置異性体の混合物となってしまう。したがって，特性解析においては，得られた修飾タンパク質について，分子量，PEGあるいは糖などの結合分子数，PEGあるいは糖などの結合部位，修飾位置異性体の構成比といった構造・組成や物理化学的性質を最新の分析法を用いて明らかにすると共に，修飾位置異性体ごとの生物学的性質についても可能な範囲で詳細な解析を行う必要がある。修飾位置異性体ごとに作用プロファイルが異なる場合，修飾位置異性体の混合物は機能面(生物活性，体内挙動)から見ても不均一な機能分子の集団となり，そのために修飾位置異性体の構成比が有効性および安全性に影響を及ぼす可能性がある。実際，PEG化インターフェロンでは，PEGの修飾位置異性体ごとに抗ウイルス活性が異なることが報告されている。また，修飾位置異性体の構成比が異なるロット間では体内動態も異なるとされている。修飾タンパク質における修飾位置異性体の解析手法としては，例えば，液体クロマトグラフィーにより異性体を分離し，それぞれのピークについて，ペプチド分析，アミノ酸配列分析，質量分析などを行うことによって，修飾部位を同定することが可能である。また，液体クロマトグラフィーの溶出パターンから異性体の構成比が分かるため，ピーク強度比を規定することで，異性体構成比の一定性が確保できる。

ここで重要なことは，前臨床，臨床試験に供した製品が，どのような不均一な分子種の集団であったか，不純物プロフィール等を明らかにすることである。前臨床，臨床試験を通して不均一性のパターンや不純物プロフィールなどの品質特性の変動がどのような範囲内であったか，その品質特性プロフィールの変動が有効性，安全性にどのように影響を及ぼしたかを精密に観察する必要がある。その結果，有効性，安全性に影響を及ぼすことがなかった品質特性プロフィールの変動の範囲が，以降，維持管理すべき製品の品質特性プロフィールの変動の範囲ということになる。当然，異性体構成比の一定性の確保や目的物質関連物質，主要な不純物に関する試験方法および規格値・判定基準は，製品の規格および試験方法の必須の項目とする必要がある。化学修飾を行う場合に製品に混入する可能性のある不純物については，製造工程由来不純物として，PEG化反応や糖付加反応などの工程で用いられる試薬やその変化物を評価項目に加える必要がある。また，目的物質由来不純物として，非結合型となった遊離のタンパク質，PEGが目的とする分子数以上に結合したdi-あるいはオリゴPEG変異体，O-結合型PEG修飾体，凝集体が混在する可能性を評価して，必要に応じて許容量に関する規格を設定すべきである。目的物質の脱アミド体や酸化体も多くのタンパク質性医薬品では，留意すべきものである。これらが，目的物質に匹敵する生物活性と安全性を有していれば目的物質関連物質として有効成分の一部を構成するが，目的物質に匹敵しない場合は目的物質由来不純物となる。

修飾反応条件が修飾部位異性体の構成比に大き

く影響し，原薬の生物活性にも影響を与える可能性が考えられることから，製品の品質の一定性を確保するためには，PEG あるいは糖など修飾条件，精製工程などは厳密に工程管理されなければならない。また，工程管理の中では，PEG あるいは糖鎖など付加反応に用いられる各種試薬の品質管理なども必要であろう。最終製品の規格および試験方法で不均一性を含む製品の品質特性プロフィール全体をカバーした十分な試験が実施できないときには，修飾条件，精製工程の工程管理や各種試薬の品質管理をより厳密に行うことで総合的に製品の品質とその恒常性を保証する必要がある。

機能性人工タンパク質の生物学的性質に関しては，天然に存在するタンパク質からの構造改変により目的以外の生物活性が変化している可能性があるため，慎重な検討が必要である。改変により意図しない変化が生じた例として，持続型のインスリン改変体であるインスリングラルギンでは，インスリン受容体との親和性はインスリンと差異がないものの，インスリン様成長因子 IGF-1 受容体との結合親和性がインスリンの 6〜8 倍であると報告されている[4]。げっ歯類を用いた 24 ヵ月間反復投与の発がん性試験により，インスリングラルギンは発がん性を有さないと判断されているが，IGF-1 受容体への高親和性結合と安全性との関連の全貌が必ずしも明らかにされたとは言えない。このような特性を持つ機能性人工タンパク質で従来の製品より医薬品としてより有用と目されるものの場合には承認を可とされたとしても，市販後安全対策(ファーマコビジランスプランニング)をしっかりとたて，市販後調査などにより安全性を慎重に観察していく必要がある。ちなみに，医薬品として実用化されているものではないが，B 鎖 10 番目の His を Asp に置換し，インスリン受容体との親和性が亢進した改変インスリンでは，ラットで乳腺腫瘍の発生が報告されている[5),6)]。1 アミノ酸の置換により発がん性が生じることを示した典型例であり，改変による生物学的性質の変化が安全性に大きく影響する場合があることを認識する必要がある。

機能性人工タンパク質の免疫原性・抗原性についても注意深い観察が必要である。一般に PEG 化タンパク質の場合には免疫原性・抗原性が減弱すると言われている。一方，アミノ酸置換体などの改変タンパク質の場合に必ず懸念されるのが，免疫原性および抗原性の問題である。タンパク質性医薬品の免疫原性や抗原性は，タンパク質の一次構造上の特徴はもとより，高次構造，製剤中の目的物質の凝集体や製造工程由来不純物，添加剤，あるいは投与経路などにも大きく影響される[7)]。通常のヒト型組換えタンパク質性医薬品でも免疫原性や抗原性が問題になる例があるが[8)]，もともとヒトには存在しない機能性人工タンパク質の場合には，その免疫原性・抗原性により一層の注意を払わねばならない。ただし，がんなどのように宿主の免疫機能が低下している患者への機能性人工タンパク質の適用と，免疫機能が過剰に亢進しているアレルギーやリウマチといった炎症性疾患への適用では，異なった免疫原性・抗原性問題への取組みやその評価基準が必要であると考えられる。またヒトに対する抗原性は一般に動物実験では評価できず，非臨床試験における評価は困難であるため，ヒトでの抗原性の予測についての方法論の確立などが望まれるところであるが，当面は治験中や市販後における注意深い臨床観察がなによりも重要であると考えられる。

5. おわりに

本節では，昨今加速度的に創出されつつある機能性人工タンパク質の品質・安全性評価の観点から，現状と将来展望，課題について論じた。ゲノミクス，トランスクリプトミクスやプロテオミクス，グライコミクス，メタボロミクスといった大規模な網羅的解析および高効率高発現・標的細胞

指向性のある遺伝子導入技術や発現制御技術，特異的評価系などによる個々の遺伝子やタンパク質の機能解析により，疾患の治癒に関わるタンパク質(医薬品シーズ・タンパク質)の探索・同定が進展し，今後益々，機能性人工タンパク質が，種々の難治性疾患に対する有用な治療薬として開発の対象となることが期待される。一方で，ウイルスや細菌のゲノム解析等の進歩も相俟って，より効率よく宿主の免疫機能を活性化したり，メモリー機能を亢進させたりするような新興・再興感染症に対する機能性人工ワクチン(抗原タンパク質)の登場も予想される。機能性人工ワクチンの場合，免疫原性・抗原性そのものが薬効となる一方で，非特異的免疫の活性化や精緻に構築されている生体免疫機構を乱すことによる思わぬ副作用が発現する可能性に十分な注意が必要となる。また，分子特性・品質特性，用法・用量や投与期間など考慮しつつ，必要に応じて上述した機能性人工タンパク質の品質・安全性確保上の課題をクリアする必要があると思われる。

参考文献

1) Kurtzhals P., Schaffer L., Sorensen A., Kristensen C., Jonassen I., Schmid C. and Trub T. : Correlations of receptor binding and metabolic and mitogenic potencies of insulin analogs designed for clinical use. Diabetes, 49 : 999-1005, 2000.

2) Yamamoto Y., Tsutsumi Y., Yoshioka Y., Nishibata T., Kobayashi K., Okamoto T., Mukai Y., Shimizu T., Nakagawa S., Nagata S. and Mayumi, T. : Site-specific PEGylation of a lysine-deficient TNF-alpha with full bioactivity. Nat. Biotechnol., 21 : 546-552, 2003.

3) Shibata H., Yoshioka Y., Ikemizu S., Kobayashi K., Yamamoto Y., Mukai Y., Okamoto T., Taniai M., Kawamura M., Abe Y., Nakagawa S., Hayakawa T., Nagata S., Yamagata Y., Mayumi T., Kamada H. and Tsutsumi, Y. : Functionalization of tumor necrosis factor-alpha using phage display technique and PEGylation improves its antitumor therapeutic window. Clin. Cancer Res., 10 : 8293-8300, 2004.

4) Walsh G. : Therapeutic insulins and their large-scale manufacture. Appl. Microbiol. Biotechnol., 67 : 151-159, 2005.

5) Dideriksen L. H., Jorgensen L. N. and Drejer, K. : Carcinogenic effect on female rats after 12 months administration of the insulin analogue B10 ASP. Diabetes, 41 : 143A, 1992.

6) Drejer K. : The bioactivity of insulin analogues from *in vitro* receptor binding to *in vivo* glucose uptake. Diabetes Metab. Rev., 8 : 259-285, 1992.

7) Schellekens H. : The immunogenicity of biopharmaceuticals. Neurology, 61 : S11-12, 2003.

8) Schllekens H. and Casadevall N. : Immunogenicity of recombinant human proteins: cause and consequences. J. Neurol., 251 (Suppl 2) : II/4-II/9, 2004.

(堤 康央／石井明子／早川堯夫)

Mini Review

Development of new anti-TNF therapy

Haruhiko Kamada *, Hiroko Shibata, and Yasuo Tsutsumi

Laboratory of Pharmaceutical Proteomics (LPP) National Institute of Biomedical Innovation (NIBIO), Osaka, Japan

We have generated the first TNFR1-selective antagonistic TNF mutant based on structural human TNF variants using our phage display technology. This TNF mutant did not activate TNFR1-mediated responses, although its affinity for TNFR1 was equivalent to human wild-type TNF (wtTNF). The TNF mutant neutralized wtTNF-induced TNFR1-mediated bioactivity without influencing TNFR2-mediated bioactivity. In hepatitis mouse models, the antagonistic TNF mutant significantly blocked liver injury caused by inflammation. These results indicate that antagonistic TNF mutants may be clinically useful for anti-TNF therapy and that phage display libraries of protein ligands can be used to select for receptor subtype-selective antagonists.

Rec.1/25/2007, Acc.4/16/2007, pp512-515

*Correspondence should be addressed to:
Haruhiko Kamada, Laboratory of Pharmaceutical Proteomics (LPP) National Institute of Biomedical Innovation (NIBIO) 7-6-8 Saito-Asagi, Ibaraki 567-0085, Osaka, Japan. Phone : +81-72-641-9811, FAX: +81-72-641-9817, e-mail: kamada@nibio.go.jp

Key words tumor necrosis factor-α, phage display system, protein mutant, TNF receptor specific antagonist, anti-TNF therapy

Inflammation is induced by physiological and chemical stimulation and is known to be mediated by the association of many biological factors. Inflammation-mediating proteins, typified by cytokines and chemokines, act in the host defense system by stimulating lymphocytes, macrophages, and endothelial cells to heal external injuries[1]. When a productive balance of these mediators collapses, inflammatory exacerbation occurs. Long-term over-expression of cytokines causes autoimmune disease[2]. Thus, development of therapeutic techniques to remedy the imbalance of cytokine production is necessary.

Tumor necrosis factor-α (TNF) is a major inflammatory cytokine and has a central role in host defense and inflammation[3]. To exert its biological function, TNF binds to two receptor subtypes, TNFR1 and TNFR2, which form homotrimers by preassembling on the cell surface[4]. Deregulation of TNF production promotes TNF-dependent pathologies and correlates with the severity and progression of inflammatory diseases such as rheumatoid arthritis (RA)[5], inflammatory bowel disease[6], septic shock[7] and hepatitis[8]. TNF blocking agents (monoclonal antibodies or soluble receptors) have shown significant clinical efficacy in certain inflammatory diseases. The major impact of TNF blocking agents on the immunological system, however, raises some concerns about the safety of this approach, especially with regard to severe infections[9], malignancies[10] and immune-mediated diseases[11]. For example, in rheumatoid arthritis and Crohn's disease, studies indicated a higher incidence of tuberculosis reactivation[12] and the induction of demyelination[13].

Although the distinction between the role of TNFR1 and TNFR2 on the immune system remains unclear, TNF secreted from activated immune cells in these diseases predominantly

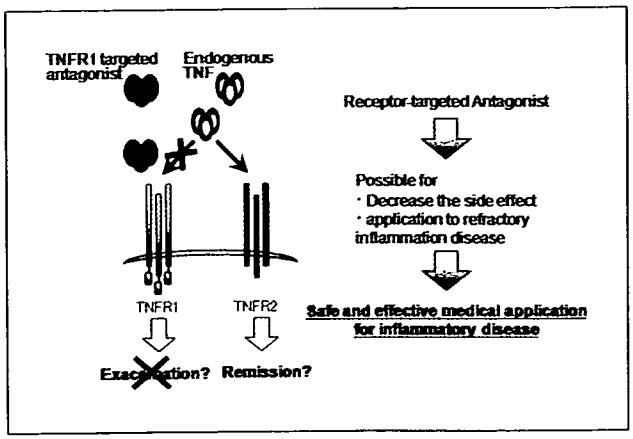

Fig.1 Generation antagonistic protein mutant for receptor targeting

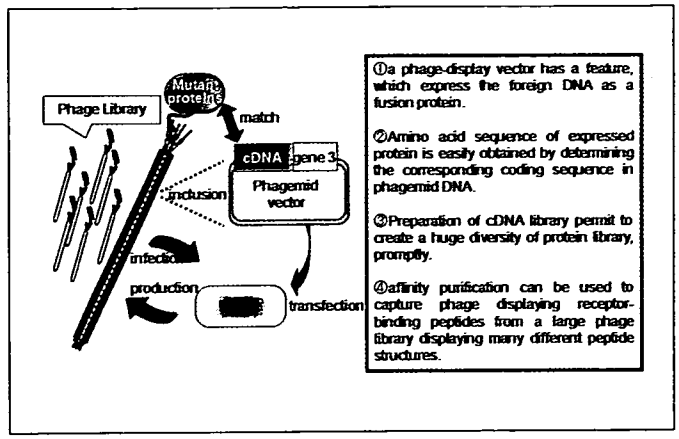

Fig.2 Benefit for engineering protein library using phage display system

activates TNFR1 and accelerates inflammation. In addition, previous studies using animal models of diseases such as arthritis[14] and hepatitis[15] indicated that mainly TNFR1 caused development and exacerbation of inflammation. Moreover, given that in mice lacking the TNFR1 the clinical course of EAE is suppressed both at the pro-inflammatory and the autoimmune phases, the TNFR1 is clearly indicated as an important target for therapy[16]. From this perspective, blocking TNFR1 signal transduction may emerge as a powerful and effective therapy for certain inflammatory diseases (Fig.1).

To develop receptor-selective protein ligands, several studies have described useful mutant proteins created by the substitution of amino acids using a site-directed mutagenesis method, as typified by Kunkel's method[17,18]. It is difficult, however, to obtain an exhaustive and functional panel of protein mutants using this mutagenesis method. Alternatively, the phage display system is a powerful *in vitro* technique that enables polypeptides with desired properties to be selected from a large collection of variants encoded by cDNAs in phagemid vectors (Fig.2). Filamentous phage display of peptide or protein variants has been widely used for rapid selection of protein variants that bind with improved affinity and specificity to target molecules[19]. The key feature of such selection schemes is that the genotype of a particular variant packaged inside a virion particle is linked to the phenotype of a displayed protein or peptide that has been fused to phage coat proteins, i.e., the gene III protein. Phage particles can be selected by binding to an affinity matrix propagated in E. coli and identified by DNA sequencing. These procedures allow phage libraries to be subjected to a selection step, called "affinity panning". Recovered clones are identified by sequencing and re-grown for further rounds of selection.

Using the phage display system, we previously isolated a lysine-deficient TNF mutant from a protein library in which all six lysine residues in the TNF molecule, including the receptor-binding site, were simultaneously replaced with other amino acids[19,20]. This strategy created novel mutant TNFs that exhibited only a slightly different mode of receptor-binding. In the present study, we used the phage display system to isolate novel TNFR1-selective antagonistic TNF mutants that efficiently inhibited a wide variety of TNFR1 mediated effects *in vitro* and *in vivo* without affecting TNFR2-mediated bioactivity.

The selection of amino acids to be altered was based on data from a point mutation study and a TNF structure-function study. Residues (amino acids 89-94) that were shown to contribute to TNFR binding were mapped onto the three-dimensional structure of human TNF. Then, these and other nearby residues were selected for randomization to generate phage libraries (Fig.3). Randomization of each of these residues was performed by PCR with mutated primers in which an NNS codon was incorporated at each randomized position. Each library contained a total of six randomized residues.

To select TNF mutants from phage library that bound strongly to human TNFR1, the mutant TNF phage library was panned against human TNFR1. As a result, we identified ten candidates as TNFR1-selective antagonists and selected the most suitable mutant that possessed the strongest antagonistic activity. To investigate the properties of this antagonistic clone, we examined the binding kinetics and binding specificities of this mutant for TNFR1 and TNFR2 using BIAcore and ELISA techniques, respectively. The antagonistic TNF mutant had an affinity for

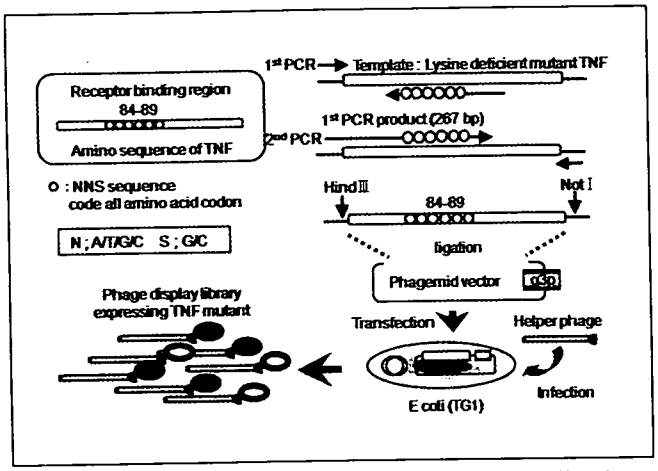

Fig.3 Engineering TNF mutant phage display library

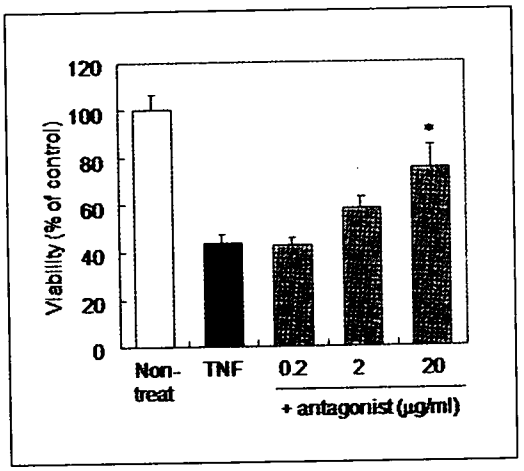

Fig.4 Inhibitory effect of antagonistic mutant TNF on TNF-induced cytotoxicity

Mouse fibrosarcoma L-M cells were treated with wild-type TNF (10 ng/ml). and serial diluted mutant TNF. After 48 hr incubation, ratio of cell death were determined by methylene blue assay.

TNFR1 equivalent to wtTNF, but almost no affinity for TNFR2. We also measured the bioactivity of the TNF mutant via TNFR-mediating response assays. The antagonistic TNF mutant bound to TNFR1 but did not transmit the death signal. To determine the ability of the TNF mutant to compete with wtTNF, we measured TNFR1-selective responses in the presence of both wtTNF and TNF mutant. The antagonistic TNF mutant inhibited wtTNF-induced cytotoxicity (Fig.4), caspase activation, and NF-κB activation through TNFR1 in a dose-dependent manner. These results suggest that the antagonistic TNF mutant is a competitive antagonist, inhibiting TNFR1-mediated pathways.

For the therapy of autoimmune disease, TNF blockades (etarnercept, as p75-IgG Fc fusion protein and lenercept as p55-IgG Fc fusion protein) have been developed. However, differences exist in the mechanisms of action of these agents that might confer risks of infection and immunogenisity. There are some reports that tuberculosis disease is a potential adverse reaction from treatment with etanercept. Moreover, antibody formation against lenercept was a significant problem which resulted in significant reduction of the half-life of the receptor. Thus, much is expected from the development of TNF receptor-selective agents that inhibit disease-causing TNF bioactivity without interfering host defense system against infection and antibody formation. In the present report, we generated a receptor-selective antagonistic TNF mutant through the use of phage display. However, there is a possibility of expressing the new function, which binds to another receptor like as TNF receptor superfamily. Therefore, the reasons of showing agonistic or antagonistic activity should be examined via structural analysis of binding sites. We are now analyzing the crystal structures of the complex formed between the antagonistic TNF mutant and TNFR1 so as to better understand the mechanisms of receptor subtype-selectivity.

While the functions of TNF and its receptors are unclear, their signaling specificities are being examined in many TNF-related studies. In this review, we studied mutant TNF antagonist that bound selectively to TNFR1. The findings from our TNFR1 and TNFR2 study are applicable to the receptors in the TNFR superfamily that do not contain a cytoplasmic death domain. However, we also have produced TNF agonist that binds to TNFR1 and TNFR2. These selective agonists and antagonists are not only therapeutically useful, but also are effective analytical tools for elucidating TNF receptor function. Further functional studies of TNF receptors could uncover interesting receptor biology and may yield additional targets for immunotherapy.

Acknowledgments

We thank Dr. Shinsaku Nakagawa and Dr. Rie Igarashi for publishing our work in this journal. This study was supported in part by Grants-in-Aid for Scientific Research (No.17689008, 17016084, 17790135, 18015055, 18659047) from the Ministry of Education, Culture, Sports, Science and Technology of Japan, in part by Health and Labor Sciences Research Grant from the Ministry of Health, Labor and Welfare of Japan, in part by Health Sciences Research Grants for Research on Health Sciences focusing on Drug Innovation from the Japan Health Sciences Foundation, in part by Takeda Science Foundation.

References

1) Tracey KJ, Cerami A: Tumor necrosis factor: a pleiotropic cytokine and therapeutic target. Annu Rev Med, 45: 491-503, 1994.
2) Cope AP: Regulation of autoimmunity by proinflammatory cytokines. Curr Opin Immunol, 10(6): 669-676, 1998.
3) Ware CF: Network communications: lymphotoxins, LIGHT, and TNF. Annu Rev Immunol, 23: 787-819, 2005.
4) Chan FK, Chun HJ, Zheng L, Siegel RM, Bui KL, Lenardo MJ: A domain in TNF receptors that mediates ligand-independent receptor assembly and signaling. Science, 288 (5475): 2351-2354, 2000.
5) Brennan FM, Feldmann M: Cytokines in autoimmunity. Curr Opin Immunol, 4(6): 754-759, 1992.
6) Van Deventer SJ: Tumour necrosis factor and Crohn's disease. Gut, 40(4): 443-448, 1997.
7) Dinarello CA, Gelfand JA, Wolff SM: Anticytokine strategies in the treatment of the systemic inflammatory response syndrome. Jama, 269(14): 1829-1835, 1993.
8) Bradham CA, Plumpe J, Manns MP, Brenner DA, Trautwein C: Mechanisms of hepatic toxicity. I.TNF-induced liver injury. Am J Physiol, 275(3 Pt 1): G387-G392, 1998.
9) Gardam MA, Keystone EC, Menzies R, Manners S, Skamene E, Long R, Vinh DC: Anti-tumour necrosis factor agents and tuberculosis risk: mechanisms of action and clinical management. Lancet Infect Dis, 3(3): 148-155, 2003.
10) Cohen RB, Dittrich KA: Anti-TNF therapy and malignancy--a critical review. Can J Gastroenterol, 15(6): 376-384, 2001.
11) Shakoor N, Michalska M, Harris CA, Block JA: Drug-induced systemic lupus erythematosus associated with etanercept therapy. Lancet, 359(9306): 579-580, 2002.
12) Keane J, Gershon S, Wise RP, Mirabile-Levens E, Kasznica J, Schwieterman WD, Siegel JN, Braun MM: Tuberculosis associated with infliximab, a tumor necrosis factor alpha-neutralizing agent. N Engl J Med, 345(15): 1098-1104, 2001.
13) Sicotte NL, Voskuhl RR: Onset of multiple sclerosis associated with anti-TNF therapy. Neurology, 57(10): 1885-1888, 2001.
14) Mori L, Iselin S, De Libero G, Lesslauer W: Attenuation of collagen-induced arthritis in 55-kDa TNF receptor type 1 (TNFR1)-IgG1-treated and TNFR1-deficient mice. J Immunol, 157(7): 3178-3182, 1996.
15) Tsuji H, Harada A, Mukaida N, Nakanuma Y, Bluethmann H, Kaneko S, Yamakawa K, Nakamura SI, Kobayashi KI, Matsushima K: Tumor necrosis factor receptor p55 is essential for intrahepatic granuloma formation and hepatocellular apoptosis in a murine model of bacterium-induced fulminant hepatitis. Infect Immun, 65(5): 1892-1898, 1997.
16) Kollias G, Kontoyiannis D: Role of TNF/TNFR in autoimmunity: specific TNF receptor blockade may be advantageous to anti-TNF treatments. Cytokine Growth Factor Rev, 13(4-5): 315-321, 2002.
17) Kunkel TA: Rapid and efficient site-specific mutagenesis without phenotypic selection. Proc Natl Acad Sci USA, 82 (2): 488-492, 1985.
18) Yamagishi J, Kawashima H, Matsuo N, Ohue M, Yamayoshi M, Fukui T, Kotani H, Furuta R, Nakano K, Yamada M: Mutational analysis of structure--activity relationships in human tumor necrosis factor-alpha. Protein Eng, 3(8): 713-719, 1990.
19) McCafferty J, Griffiths AD, Winter G, Chiswell DJ: Phage antibodies: filamentous phage displaying antibody variable domains. Nature, 348(6301): 552-554, 1990.
20) Shibata H, Yoshioka Y, Ikemizu S, Kobayashi K, Yamamoto Y, Mukai Y, Okamoto T, Taniai M, Kawamura M, Abe Y, Nakagawa S, Hayakawa T, Nagata S, Yamagata Y, Mayumi T, Kamada H, Tsutsumi Y: Functionalization of tumor necrosis factor-alpha using phage display technique and PEGylation improves its antitumor therapeutic window. Clin Cancer Res, 10(24): 8293-8300, 2004.

nature medicine

Central control of bone remodeling by neuromedin U

Shingo Sato[1], Reiko Hanada[2], Ayako Kimura[1], Tomomi Abe[3], Takahiro Matsumoto[4,5], Makiko Iwasaki[1], Hiroyuki Inose[1], Takanori Ida[2], Michihiro Mieda[3], Yasuhiro Takeuchi[6], Seiji Fukumoto[7], Toshiro Fujita[7], Shigeaki Kato[4,5], Kenji Kangawa[8], Masayasu Kojima[2], Ken-ichi Shinomiya[1] & Shu Takeda[1]

Bone remodeling, the function affected in osteoporosis, the most common of bone diseases, comprises two phases: bone formation by matrix-producing osteoblasts[1] and bone resorption by osteoclasts[2]. The demonstration that the anorexigenic hormone leptin[3–5] inhibits bone formation through a hypothalamic relay[6,7] suggests that other molecules that affect energy metabolism in the hypothalamus could also modulate bone mass. Neuromedin U (NMU) is an anorexigenic neuropeptide that acts independently of leptin through poorly defined mechanisms[8,9]. Here we show that *Nmu*-deficient (*Nmu*$^{-/-}$) mice have high bone mass owing to an increase in bone formation; this is more prominent in male mice than female mice. Physiological and cell-based assays indicate that NMU acts in the central nervous system, rather than directly on bone cells, to regulate bone remodeling. Notably, leptin- or sympathetic nervous system–mediated inhibition of bone formation[6,7] was abolished in *Nmu*$^{-/-}$ mice, which show an altered bone expression of molecular clock genes (mediators of the inhibition of bone formation by leptin). Moreover, treatment of wild-type mice with a natural agonist for the NMU receptor decreased bone mass. Collectively, these results suggest that NMU may be the first central mediator of leptin-dependent regulation of bone mass identified to date. Given the existence of inhibitors and activators of NMU action[10], our results may influence the treatment of diseases involving low bone mass, such as osteoporosis.

Bone mass is maintained at a constant level between puberty and menopause by a succession of bone-resorption and bone-formation phases[11,12]. The discovery that neuronal control of bone remodeling is mediated by leptin[6] shed light on a new regulatory mechanism of bone remodeling and also suggested that bone mass may be regulated by a variety of neuropeptides[13]. In line with this observation, cannabinoids and pituitary hormones have been shown to be intimately involved in bone remodeling[14,15]. Leptin inhibits bone formation by binding to its receptors located in hypothalamus and thereby activating the sympathetic nervous system (SNS), which requires the adrenergic β2 receptors (Adrb2) expressed in osteoblasts[7,16]. Downstream of Adrb2, leptin signaling activates molecular clock genes that regulate osteoblast proliferation and hence bone formation[17]. In addition, leptin regulates bone resorption through two distinct pathways[16].

NMU is a small peptide produced by nerve cells in the submucosal and myenteric plexuses in the small intestine, and also by structures in the brain, including the dorsomedial nucleus of the hypothalamus[9]. It is generally assumed that NMU acts as a neuropeptide to regulate various aspects of physiology, including appetite, stress response and SNS activation[9]. Indeed, NMU-deficient (*Nmu*$^{-/-}$) mice develop obesity due to increased food intake and reduced locomotor activity that is believed, at least in part, to be leptin independent[8]. In addition, expression of NMU is diminished in leptin-deficient (*Lep*^{ob}) mice[18], but can be induced in these mice by leptin treatment[19]. In search of additional neuropeptides that regulate bone remodeling, we analyzed *Nmu*$^{-/-}$ mice.

When assessed at 3 and 6 months of age, both male and female *Nmu*$^{-/-}$ mice showed a high bone mass phenotype as compared to the wild type (WT), with male mice more severely affected than female mice (**Fig. 1a** and data not shown). The presence of a uniform increase in bone mineral density (BMD) along the femurs of *Nmu*$^{-/-}$ mice suggested that both trabecular and cortical bone were equally affected (**Supplementary Fig. 1** online). Microcomputed tomography analysis confirmed this observation (**Fig. 1b,c**). To determine whether this phenotype was secondary to the obesity of the *Nmu*$^{-/-}$ mice, we restricted their food intake for 1 month starting at 2 months of age. This manipulation normalized the body weight and serum insulin level of the *Nmu*$^{-/-}$ mice but did not affect their high bone mass phenotype (**Fig. 1d** and data not shown). Of note, when *Nmu*$^{-/-}$ mice were backcrossed to the C57BL/6J genetic background, their body weight became similar to that of their WT littermates; however, their BMD remained high (data not shown). These results suggest that NMU regulates bone mass independently of its regulation of energy metabolism, just as leptin does[7]. To better characterize the cellular nature of the bone phenotype in the *Nmu*$^{-/-}$ mice, we

[1]Department of Orthopaedic Surgery, Graduate School, 21st Century Center of Excellence Program, Tokyo Medical and Dental University, 1-5-45 Yushima, Bunkyo-ku, Tokyo 113-8519, Japan. [2]Division of Molecular Genetics, Institute of Life Science, Kurume University, 1-1 Hyakunen-kohen, Kurume, Fukuoka 839-0842, Japan. [3]Department of Molecular Neuroscience, Tokyo Medical and Dental University 1-5-45 Yushima, Bunkyo-ku, Tokyo 113-8519, Japan. [4]Institute of Molecular and Cellular Biosciences, University of Tokyo, 1-1-1 Yayoi, Bunkyo-ku, Tokyo 113-0032, Japan. [5]Exploratory Research for Advanced Technology, Japan Science and Technology Agency, 4-1-8 Honcho, Kawaguchi, Saitama 332-0012, Japan. [6]Toranomon Hospital Endocrine Center, 2-2-2 Toranomon, Minato-ku, Tokyo 105-8470, Japan. [7]Division of Nephrology and Endocrinology, Department of Internal Medicine, University of Tokyo Hospital, 7-3-1 Hongo, Bunkyo-ku, Tokyo 113-8655, Japan. [8]Department of Biochemistry, National Cardiovascular Center Research Institute, 5-7-1 Fujishiro-dai, Suita-shi, Osaka 565-8565, Japan. Correspondence should be addressed to S.T. (shu-tky@umin.ac.jp).

Received 4 June; accepted 8 August; published online 16 September 2007; doi:10.1038/nm1640

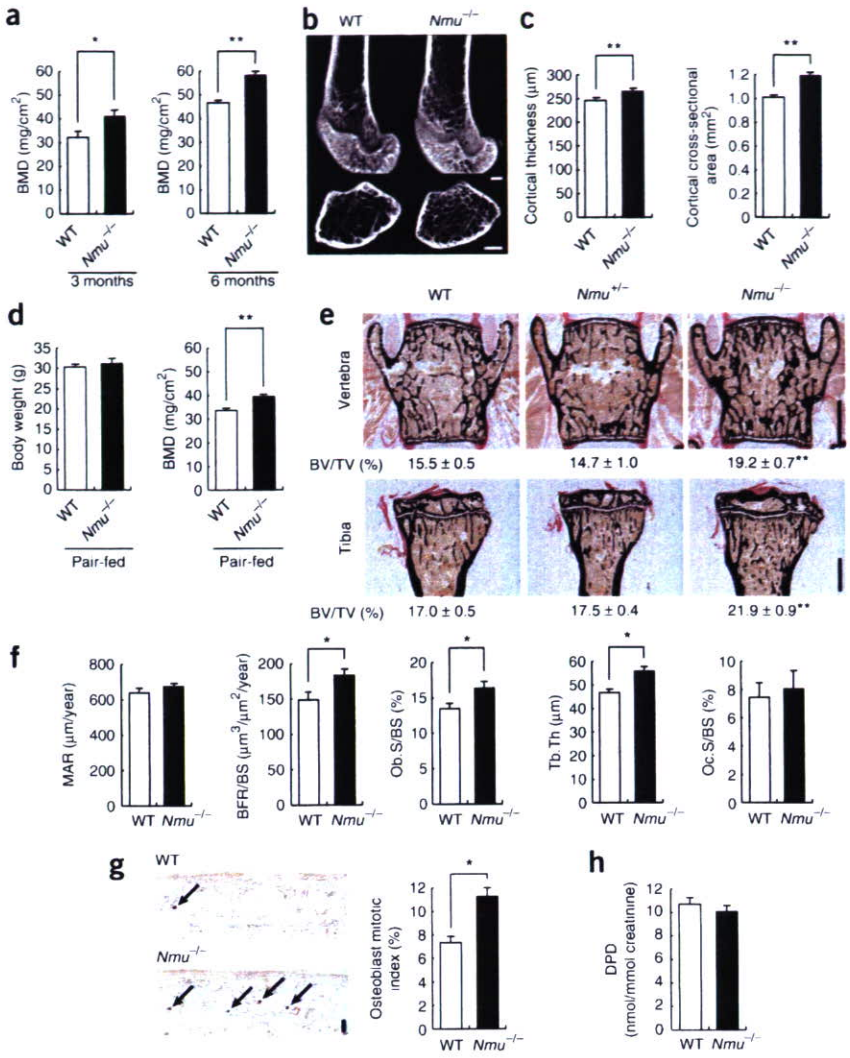

Figure 1 High bone mass in *Nmu*$^{-/-}$ mice due to increased bone formation. (**a**) Bone mineral density (BMD) of the femurs of 3 (left)- and 6 (right)-month-old male wild-type (WT) and *Nmu*$^{-/-}$ mice. (**b**) Micro-computed tomography (μCT) analysis of the distal femurs of male mice at 3 months. Scale bars, 500 μm. (**c**) Cortical thickness and cross-sectional area of the femurs of 3-month-old male mice. (**d**) Body weight and BMD of 3-month-old male mice with restricted food intake. (**e**) Histological analysis of the vertebrae and tibiae of 3-month-old male WT, *Nmu*$^{+/-}$ and *Nmu*$^{-/-}$ mice. Bone volume per tissue volume (BV/TV). Scale bars, 1 mm. (**f**) Histomorphometric analysis of the vertebrae of 3-month-old male mice. Mineral apposition rate (MAR), bone formation rate over bone surface area (BFR/BS), osteoblast surface area over bone surface area (Ob.S/BS), trabecular thickness (Tb. Th) and osteoclast surface area over bone surface area (Oc.S/BS). (**g**) Increased osteoblast proliferation in newborn *Nmu*$^{-/-}$ mice. Immunolocalization of BrdU incorporation (arrows) in the calvariae of WT and *Nmu*$^{-/-}$ mice (left). Osteoblast mitotic index (right). Scale bar, 20 μm. (**h**) Urinary elimination of deoxypyridinoline (DPD) in WT and *Nmu*$^{-/-}$ mice. **, $P < 0.01$; *, $P < 0.05$.

performed histological and histomorphometric analyses of vertebrae and tibiae in both male and female animals (**Fig. 1e** and **Supplementary Fig. 1**). At 3 and 6 months of age, *Nmu*$^{-/-}$ mice showed greater bone volume in both vertebrae and tibiae than did WT littermates, with male mice having a more pronounced phenotype (**Fig. 1e** and **Supplementary Fig. 1**). At the present time we do not have a clear explanation of the difference in phenotype severity between male and female mice. Bone formation rates (WT mice, 146.9 ± 12.3, *Nmu*$^{-/-}$ mice, 183.7 ± 10.3, $P < 0.05$) and osteoblast numbers were both significantly greater in the vertebrae and tibiae of *Nmu*$^{-/-}$ mice (**Fig. 1f** and **Supplementary Fig. 1**). The higher osteoblast numbers in the presence of a normal mineral apposition rate (**Fig. 1f** and **Supplementary Fig. 1**), which reflects the function of individual osteoblasts[20], suggested that osteoblast proliferation may be increased in *Nmu*$^{-/-}$ mice. Indeed, 5-bromo-2-deoxyuridine (BrdU)-positive proliferative osteoblast counts were significantly increased in *Nmu*$^{-/-}$ mice *in vivo* (**Fig. 1g**), demonstrating that NMU affects osteoblast proliferation. In contrast, *Nmu*$^{-/-}$ and WT mice showed comparable osteoclast numbers and osteoclast surface areas (**Fig. 1f** and **Supplementary Fig. 1**), suggesting that NMU does not affect bone resorption. This observation was further supported by the normal level of urinary elimination of deoxypyridinoline in *Nmu*$^{-/-}$ mice (**Fig. 1h**).

Taken together, these results demonstrate that NMU deficiency results in an isolated increase in bone formation leading to high bone mass. *Nmu*-heterozygote mice did not have an overt bone abnormality at any age analyzed (**Fig. 1e**).

Two cognate G protein–coupled receptors have been reported to be NMU receptors: NMUR1, which is expressed in various tissues, including the small intestine and lung (data not shown), and NMUR2, which is predominantly expressed in the hypothalamus and the small intestine (**Fig. 2a**)[18]. Both receptors and NMU itself were barely detectable in bone (**Fig. 2a**). To further exclude the possibility of a direct action of NMU on osteoblasts, we treated mouse primary osteoblasts with varying concentrations of NMU. Alkaline phosphatase activity, mineralization and expression of osteoblastic genes were all unaffected by this treatment (**Fig. 2b,c**). In addition, there were no differences between WT mice and *Nmu*$^{-/-}$ mice in the expression of osteoblastic genes *in vivo* (**Fig. 2d**). Moreover, both WT and *Nmu*$^{-/-}$ osteoblasts proliferated normally *in vitro* in response to NMU treatment (**Fig. 2e**), though *Nmu*$^{-/-}$ osteoblasts proliferated more than WT osteoblasts *in vivo* (**Fig. 1g**). Osteoclastic differentiation from bone marrow macrophages was unchanged by NMU treatment (**Fig. 2f**), as expected from the absence of a bone resorption defect *in vivo* (**Fig. 1f,h**). Taken together, these results strongly suggest that NMU's effect on bone may not come from its direct action on osteoblasts, but rather through another relay.

Because the anorexigenic effect of NMU requires a hypothalamic relay[8,19] and because hypothalamic neurons have been shown to regulate bone mass, we tested whether NMU's regulation of bone formation could involve a central relay. Continuous intracerebroventricular (i.c.v.) infusion of NMU into *Nmu*$^{-/-}$ mice decreased their fat mass and fat pad weight significantly, although body weight was not

affected (**Fig. 2g** and **Supplementary Fig. 2** online). In addition, NMU i.c.v. infusion eliminated the high bone mass phenotype in *Nmu*$^{-/-}$ mice (**Fig. 2g** and **Supplementary Fig. 2**), suggesting that NMU inhibits bone formation through the central nervous system.

The central nature of bone remodeling regulation by NMU, along with the notion that the anorexigenic effect of NMU may be independent of leptin[8], prompted us to examine whether leptin could be involved in the regulation of bone formation by NMU. To address this question, we performed i.c.v. infusion of NMU or leptin in *Lep*^{ob} mice. NMU decreased fat pad weight significantly, albeit to a milder extent than that achieved by leptin (**Fig. 3a** and **Supplementary Fig. 3** online). Body weight was not significantly changed by the NMU infusion, indicating that this treatment had only a mild effect on energy metabolism (data not shown). In contrast, NMU decreased bone mass in *Lep*^{ob} mice as efficiently as leptin did (**Fig. 3a**). These results indicate that NMU inhibits bone formation in a leptin-independent manner. Next, we asked whether leptin could correct the high bone mass phenotype of *Nmu*$^{-/-}$ mice. Leptin i.c.v. infusion decreased bone volume and bone formation in WT mice, as previously reported (**Fig. 3b** and **Supplementary Fig. 3**)[6]. However, the leptin paradoxically increased bone volume and osteoblast number in *Nmu*$^{-/-}$ mice (**Fig. 3b,c** and **Supplementary Fig. 3**). The fact that leptin decreased fat mass and fat pad weight in *Nmu*$^{-/-}$ mice and increased urinary elimination of normetanephrine, a metabolite of noradrenaline[17], verified that the administration of leptin was properly performed (**Fig. 3b,d** and **Supplementary Fig. 3**). Therefore, taken together, these results suggest that NMU acts downstream of leptin to regulate bone formation.

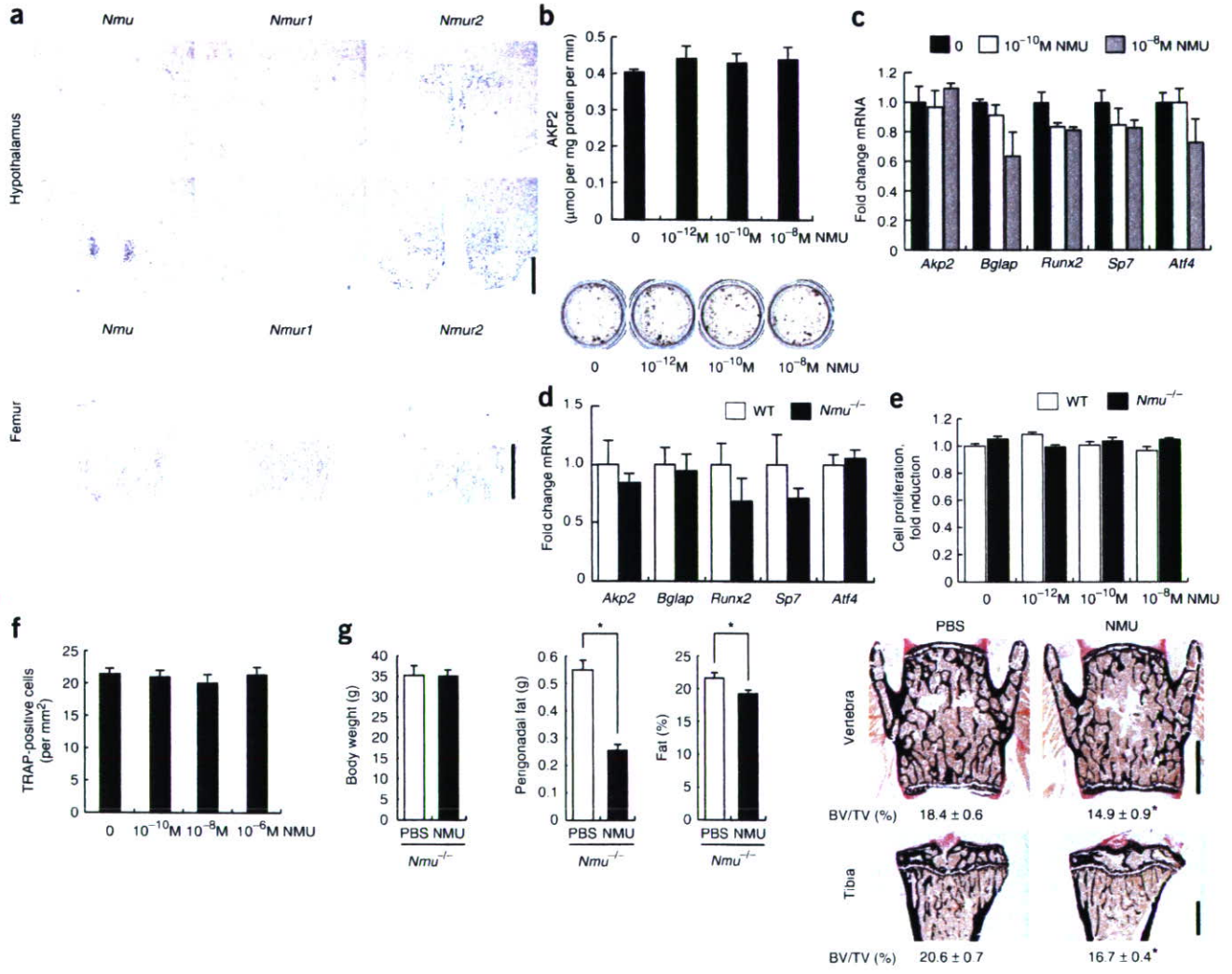

Figure 2 Absence of NMU's direct effect on osteoblasts; decrease in bone mass by NMU i.c.v. infusion. (**a**) Expression of *Nmu*, *Nmur1* and *Nmur2* in the hypothalamus at the atlas-levels of 38 (top) and 43 (bottom) and in the femur as shown by *in situ* hybridization. Note the expression of *Nmu* in the dorsomedial nucleus of the hypothalamus (DMH) (bottom) and *Nmur2* in paraventricular nucleus (top), arcuate nucleus and DMH (bottom). Scale bars, 500 μm. (**b–d**) Effect of NMU on osteoblast differentiation. (**b,c**) WT osteoblasts treated with NMU. (**b**) Alkaline phosphatase (AKP2) activity (top), mineralized nodule formation (bottom). (**c**) Expression of osteoblastic genes (*Akp2*, *Bglap*, *Runx2*, *Sp7* and *Atf4*), depicted as fold change over WT expression. (**d**) Expression of osteoblastic genes in WT and *Nmu*$^{-/-}$ femurs. (**e**) Effect of NMU on osteoblast proliferation. WT or *Nmu*$^{-/-}$ osteoblasts treated with NMU. (**f**) Effect of NMU on osteoclast differentiation. Bone marrow–derived osteoclasts treated with NMU. (**g**) Effect of NMU i.c.v. infusion on body weight, fat pad weight (perigonadal fat) and fat mass (left). Histological analysis of the vertebrae (top right) and tibiae (bottom right). Male mice at 3 months of age were used. Scale bars, 1 mm. *, $P < 0.05$.

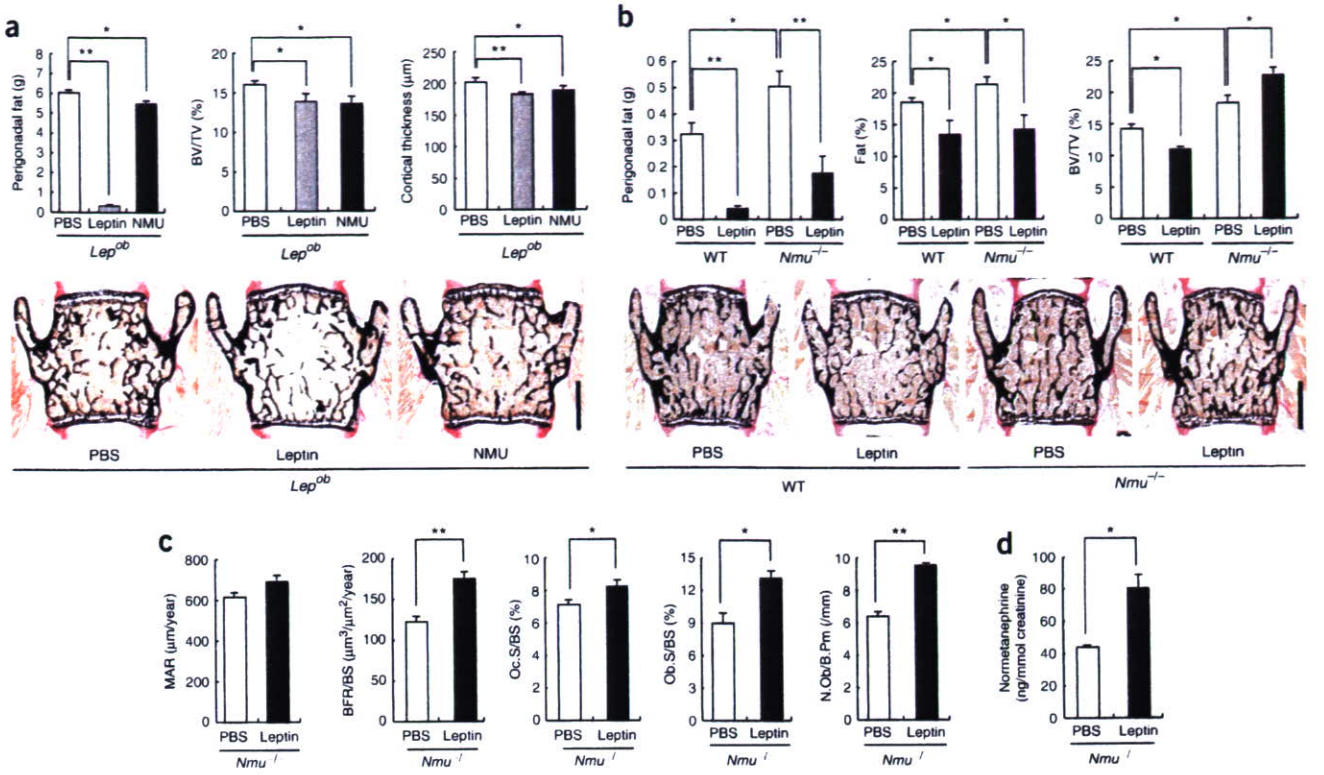

Figure 3 Leptin does not eliminate high bone mass in *Nmu*$^{-/-}$ mice. (**a**) Effect of NMU or leptin i.c.v. infusion in *Lep*^{ob} mice (3-month-old males). Fat pad weight and bone mass were determined by histology and cortical thickness by μCT analysis. (**b–d**) Effect of leptin i.c.v. infusion on *Nmu*$^{-/-}$ mice (3-month-old males). (**b**) Fat pad weight, fat mass and bone mass shown by histology. (**c**) Histomorphometric analysis. N. Ob/B.Pm indicates the number of osteoblasts per bone perimeter. (**d**) Urinary elimination of normetanephrine. Scale bars, 1 mm. **, $P < 0.01$; *, $P < 0.05$.

The SNS is a major mediator of leptin's antiosteogenic action[7]. NMUR2 is expressed in paraventricular nuclei, whose neurons directly project to the sympathetic preganglionic neurons, and NMU stimulates sympathetic outflow[9,21]. These observations, along with the fact that *Nmu*$^{-/-}$ mice have osteoblastic defects similar to the one observed in *Adrb2*-deficient mice[16], prompted us to explore whether NMU and sympathetic tone are in the same pathway regulating bone formation. Indeed, *Nmu/Adrb2* double heterozygote mice had higher bone mass than *Adrb2* single heterozygote mice (**Fig. 4a**), although *Nmu* single heterozygote mice had normal bone mass (**Fig. 1e** and **Supplementary Fig. 1**). Given that *Nmu* expression in the hypothalamus was reduced in *Nmu* single heterozygote mice (data not shown), compound heterozygosity of *Nmu* and *Adrb2* may have resulted in higher bone mass. Furthermore, this result suggests that these two pathways share a common molecule. Of note, *Nmu*$^{-/-}$ mice had a higher degree of urinary elimination of normetanephrine than WT littermates (**Fig. 4b**), which would decrease bone mass, yet they had high bone mass. This suggests that their high bone mass phenotype is not caused by decreased SNS activity, but is instead the result of resistance to the antiosteogenic activity of the SNS. This is in agreement with the observation that i.c.v. infusion of leptin, a potent stimulator of SNS activity, did not decrease bone mass in *Nmu*$^{-/-}$ mice (**Fig. 3b** and **Supplementary Fig. 3**). Furthermore, injection of isoproterenol, a sympathomimetic, reduced bone mass in WT mice[7] but not in *Nmu*$^{-/-}$ mice (**Fig. 4c** and **Supplementary Fig. 4** online). Thus, *Nmu*$^{-/-}$ mice are resistant to the antiosteogenic effects of both leptin and the SNS.

We present six experimental arguments to strongly suggest that the failure of leptin or isoproterenol to decrease bone mass in *Nmu*$^{-/-}$ mice is not due to leptin-SNS signaling defects. First, leptin infusion decreased fat pad weight equally well in WT and in *Nmu*$^{-/-}$ mice and could increase normetanephrine abundance in *Nmu*$^{-/-}$ mice (**Fig. 3b,d** and **Supplementary Fig. 3**). Second, the expression of *Adrb2* was not different in WT and *Nmu*$^{-/-}$ bones (**Fig. 4d**). Third, treatment with NMU did not affect *Adrb2* expression in osteoblasts (**Supplementary Fig. 5** online). Fourth, isoproterenol induced expression of *Tnfsf11* (encoding tumor necrosis factor superfamily, member 11) and decreased expression of *Tnfrsf11b* (encoding tumor necrosis factor superfamily, member 11b, also known as osteoprotegerin), *Runx2* (encoding runt-related transcription factor-2) and *Col1a1* (encoding collagen type I), molecular markers for the effect of SNS activation on osteoblasts, in both WT and *Nmu*$^{-/-}$ osteoblasts (**Fig. 4d**). Fifth, isoproterenol induced cAMP production equally well in WT and *Nmu*$^{-/-}$ osteoblasts (**Fig. 4e**). Sixth, and most notably, leptin increased bone resorption to a similar extent in WT and *Nmu*$^{-/-}$ mice (**Fig. 3c** and **Supplementary Fig. 3**).

The fact that the leptin-SNS pathway is intact in *Nmu*$^{-/-}$ mice, together with the paradoxical increase in osteoblast number induced by leptin i.c.v. infusion in *Nmu*$^{-/-}$ mice (**Fig. 3c**), suggests that NMU affects only the negative regulator of bone remodeling by leptin, that is, the molecular clock. Indeed, the expression of *Per1* and *Per2* (encoding period homolog-1 and -2, respectively) was downregulated in *Nmu*$^{-/-}$ bones as compared to WT bones (**Fig. 4f** and **Supplementary Fig. 6** online). Thus, NMU, acting through the central nervous system, affects the molecular clock in bone.

Because bone resorption in *Nmu*$^{-/-}$ mice was comparable to that in the wild type, despite the high SNS activity in these mice, we also

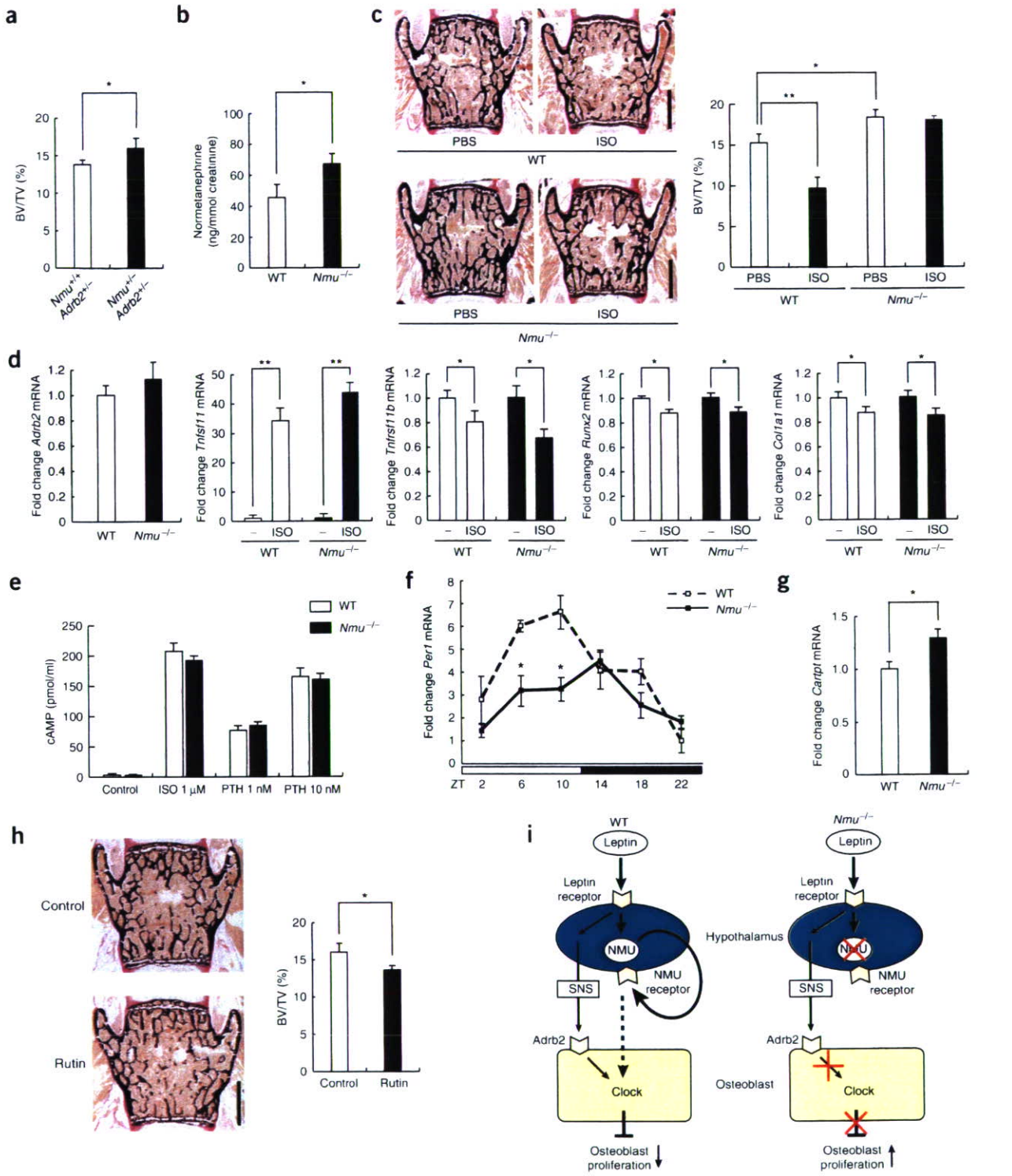

Figure 4 Sympathetic activation does not rescue high bone mass in *Nmu*$^{-/-}$ mice. (**a**) Bone mass in *Adrb2*$^{+/-}$ /*Nmu*$^{+/-}$ and *Adrb2*$^{+/-}$ /*Nmu*$^{+/+}$ mice as determined by histology (3-month-old males). (**b**) Increased urinary elimination of normetanephrine in *Nmu*$^{-/-}$ mice. (**c**) Effect of sympathetic activation by isoproterenol (ISO) injection in *Nmu*$^{-/-}$ mice (3-month-old males). Shown is the bone mass of vertebrae as determined by histology. (**d**) Expression of *Adrb2* in the femurs of WT and *Nmu*$^{-/-}$ mice (left). Gene expression changes induced by isoproterenol (ISO) treatment of WT and Nmu$^{-/-}$ osteoblasts (four rightmost graphs). (**e**) cAMP concentration in the culture medium of WT and *Nmu*$^{-/-}$ osteoblasts after ISO treatment. Parathyroid hormone (PTH) was used as a control. (**f**) Expression of *Per1* in the femurs of WT and *Nmu*$^{-/-}$ mice. Zeitberger time (ZT) is indicated on the *x*-axis. (**g**) Expression of *Cartpt* in the hypothalamus of WT and *Nmu*$^{-/-}$ mice. (**h**) Rutin decreases bone mass in WT mice as determined by histological analysis of vertebrae (left) and quantitative histomorphometric analysis (right) (3-month-old males). Scale bar, 1 mm. **, $P < 0.01$; *, $P < 0.05$. (**i**) Model of leptin, sympathetic nervous system (SNS) and NMU signaling for the regulation of bone formation in WT mice (left) and *Nmu*$^{-/-}$ mice (right).

tested whether the expression of *Cartpt* (encoding cocaine- and amphetamine-regulated transcript propeptide), a central mediator of leptin's action on bone resorption[16], was altered in these mice. Indeed, *Cartpt* expression was increased in *Nmu*$^{-/-}$ mice as compared to WT littermates (**Fig. 4g** and **Supplementary Fig. 7** online). These results suggest that the protective activity of Cart on bone resorption compensates for the bone-resorbing activity induced by the SNS in *Nmu*$^{-/-}$ mice. The effect of other leptin-regulated neuropeptides, such as NPY (neuropeptide Y), AgRP (agouti-related protein) and α-MSH (α-melanotropin), will be limited, because the expression of *Npy* and *Agrp* was unchanged in *Nmu*$^{-/-}$ mice[8] and melanocortin 4 receptor, a major receptor for α-MSH, has been shown to have little effect on bone remodeling by itself[22].

Lastly, we treated WT mice with rutin, a natural NMUR2 agonist found in daily foods such as buckwheat[23]. Consistent with the high bone mass phenotype of the *Nmu*$^{-/-}$ mice, rutin decreased bone mass significantly in WT mice (**Fig. 4h**). This result, together with the predominant expression of *Nmur2* in the hypothalamus (**Fig. 2a**), suggests that NMU regulates bone remodeling through NMUR2.

Collectively, these results suggest that NMU, through a central relay and via an unidentified pathway, acts as a modulator of leptin-SNS-Adrb2 regulation of bone formation (**Fig. 4i**). However, one concern still remains: because leptin affects several pathways originating in the hypothalamus and elsewhere in the brain, i.c.v. infusion of leptin may have resulted in an uncoordinated change in leptin-regulated bone remodeling that does not reflect a physiological role of leptin. To rigorously address that question, an analysis of a mouse model in which a specific nucleus of the hypothalamus is activated by leptin will be necessary. From a therapeutic point of view, given the lack of an obesity phenotype in *Nmur2*-deficient mice[24], an NMU antagonist may be a candidate for the treatment of bone-loss disorders without inducing unwanted body weight gain.

METHODS

Animals. *Nmu*$^{-/-}$ and *Adrb2*$^{-/-}$ mice were previously described[8,16]. We purchased C57BL/6J mice and C57BL/6J *Lep*^{ob} from the Jackson Laboratory. We maintained all of the mice under a 12 hr light-dark cycle with *ad libitum* access to regular food and water, unless specified. For pair-fed experiments, we caged *Nmu*$^{-/-}$and WT mice individually for 12 weeks as described[8]. In brief, *Nmu*$^{-/-}$ mice were given access to water *ad libitum* and fed the amount of chow eaten on the previous day by a WT littermate. We determined mouse genotypes by PCR as previously described[8,16]. We injected isoproterenol (10 mg/kg, Sigma) intraperitoneally (i.p.) once daily for 4 weeks. Rutin (Sigma) was administered orally 300 mg per kg body weight per day for 4 weeks. All animal experiments were performed with the approval of the Animal Study Committee of Tokyo Medical and Dental University and conformed to relevant guidelines and laws.

Dual X-ray absorptiometry and microcomputed tomography analysis. We measured bone mineral density (BMD) of the femurs and fat pad composition by DCS–600 (Aloka). We obtained two-dimensional images of the distal femurs by microcomputed tomography (μCT, Comscan). We measured cortical thickness and cross-sectional area at the center of the femur. We examined at least eight mice for each group.

Histological and histomorphometric analysis. We injected calcein (25 mg/kg, Sigma) i.p. 5 and 2 d before sacrifice. We stained undecalcified sections of the third and fourth lumbar vertebrae and tibiae with von Kossa staining. We performed static and dynamic histomorphometric analyses using the Osteomeasure Analysis System (Osteometrics). We analyzed 8–10 mice for each group.

***In situ* hybridization analysis.** We performed *in situ* hybridization analysis according to the established protocol[25]. Antisense cRNA probe for *Cartpt* was previously described[26]. We used fragments of cDNA for *Nmu* (105 base pairs upstream to 647 base pairs downstream of the initiation codon), *Nmur1* (13–1242 base pairs downstream of the initiation codon) and *Nmur2* (16–1252 base pairs downstream of the initiation codon) to generate antisense probes. We stained sections hybridized with ^{35}S-labeled probes with Hoechst 33528 and quantitatively analyzed the expression of *Cartpt* with a phosphorimager (Bass–2500, Fuji). The atlas-level of designations corresponds to those described previously[27]. We analyzed six mice for each group.

Measurement of deoxypyridinoline cross-links and normetanephrine. We measured urinary deoxypyridinoline cross-links (DPD) and normetanephrine with the METRA DPD-EIA kit (Quidel) and the Normetanephrine-ELISA kit (ALPCO), respectively, according to the manufacturer's instructions. We used creatinine values to standardize between samples (Creatinine Assay Kit, Cayman). We examined eight samples for each group.

Cell culture. *In vitro* primary osteoblast cultures were established as previously described[6]. Briefly, we cultured primary osteoblasts from calvariae of 4-d-old mice in α-MEM (Sigma) containing ascorbic acid (0.1 mg/ml, Sigma). We added NMU to the medium twice daily. After 14 d, we measured alkaline phosphatase activity with the ALP kit (Wako). For the mineralization assay, we supplemented the medium with β-glycerophosphate (5 mM, Sigma). We assessed mineralized nodule formation by von Kossa staining. We performed the cell proliferation and cAMP assays with the Cell Proliferation Assay (Promega) and cAMP EIA kit (Cayman Chemical), respectively. *In vitro* osteoclast differentiation has been described previously[16]. Briefly, bone marrow cells of 2-month-old mice were cultured in the presence of human macrophage colony-stimulating factor (10 ng/ml, R&D Systems) for 2 d and then differentiated into osteoclasts with human RANKL (50 ng/ml, Peprotech) and human macrophage colony-stimulating factor (10 ng/ml) for 3 d. We counted tartrate-resistant acid phosphatase (TRAP)-positive multinucleated cells (more than 3 nuclei). We performed all the cell cultures in triplicate or quadruplicate wells and repeated more than 3 times.

BrdU immunohistochemistry. For BrdU labeling, we injected 100 μg BrdU i.p. into 3-d-old mice 1 h before sacrifice. We embedded calvariae in paraffin and cut coronally. We detected BrdU-incorporated osteoblasts with the BrdU Immunohistochemistry Kit (Exalpha Biologicals). We calculated the number of BrdU-positive osteoblasts over the total number of osteoblasts (osteoblast mitotic index) at three different locations (+3.0, 3.5 and 4.0 AP (0 point: bregma)) per mouse. We analyzed six mice per group.

Intracerebroventricular infusion. Intracerebroventricular infusion was performed as previously described[6]. Briefly, we exposed the calvaria of an anesthetized mouse, implanted a 28-gauge cannula (Plastics ONE) into the third ventricle and then connected the cannula to an osmotic pump (Durect) placed in the dorsal subcutaneous space of the mouse. We infused rat Neuromedin U-23 (Peptide Institute) or human leptin (Sigma) at 0.125 nmol/hr or 8 ng/hr, respectively, for 28 d.

Quantitative RT–PCR analysis. After flushing mouse bone marrow out of the bone with PBS, we extracted bone RNA with Trizol (Invitrogen) and performed reverse transcription for cDNA synthesis. We performed quantitative analysis of gene expression with the Mx3000P real-time PCR system (Stratagene). Primer sequences are available upon request. We used GAPDH expression as an internal control.

Statistical analysis. All data are represented as mean ± s.d. ($n = 8$ or more). We performed statistical analysis by Student's *t*-test. Values were considered statistically significant at $P < 0.05$. Results are representative of more than four individual experiments.

Note: Supplementary information is available on the Nature Medicine website.

ACKNOWLEDGMENTS

We thank G. Karsenty, M. Patel and P. Ducy for critical review of the manuscript and for helpful discussions; K. Nakao, M. Noda, T. Matsumoto and S. Ito for insightful suggestions; P. Barrett (Rowett Research Institute, UK) for providing a plasmid for the *Cartpt* probe; and J. Chen, M. Starbuck, S. Sunamura, H. Murayama, H. Yamato, and M. Kajiwara for technical assistance. This work was supported by grant-in-aid for scientific research from the Japan Society for

the Promotion of Science, a grant for the 21st Century Center of Excellence program from the Ministry of Education, Culture, Sports, Science, and Technology of Japan, Ono Medical Research Foundation, Yamanouchi Foundation for Research on Metabolic Disorders, Kanae Foundation for the Promotion of the Medical Science and the Program for Promotion of Fundamental Studies in Health Sciences of the National Institute of Biomedical Innovation of Japan.

AUTHOR CONTRIBUTIONS

S. Sato conducted most of the experiments. K. Kangawa and M. Kojima generated *Nmu*$^{-/-}$ mice. R. Hanada and T. Ida conducted *in vitro* experiments. S. Fukumoto, Y. Takeuchi and T. Fujita contributed by conducting dual X-ray absorptiometry analyses and providing suggestions on the project. M. Iwasaki prepared the constructs. A. Kimura performed i.c.v. infusion experiments. H. Inose conducted μCT analyses. T. Matsumoto and S. Kato conducted histological analyses for brain tissue. T. Abe and M. Mieda performed *in situ* hybridization analysis. S. Takeda and K. Shinomiya designed the project. S. Takeda supervised the project and wrote most of the manuscript.

Published online at http://www.nature.com/naturemedicine
Reprints and permissions information is available online at http://npg.nature.com/reprintsandpermissions

1. Rodan, G.A. & Martin, T.J. Therapeutic approaches to bone diseases. *Science* **289**, 1508–1514 (2000).
2. Teitelbaum, S.L. & Ross, F.P. Genetic regulation of osteoclast development and function. *Nat. Rev. Genet.* **4**, 638–649 (2003).
3. Saper, C.B., Chou, T.C. & Elmquist, J.K. The need to feed: homeostatic and hedonic control of eating. *Neuron* **36**, 199–211 (2002).
4. Ahima, R.S. & Flier, J.S. Leptin. *Annu. Rev. Physiol.* **62**, 413–437 (2000).
5. Spiegelman, B.M. & Flier, J.S. Obesity and the regulation of energy balance. *Cell* **104**, 531–543 (2001).
6. Ducy, P. *et al.* Leptin inhibits bone formation through a hypothalamic relay: a central control of bone mass. *Cell* **100**, 197–207 (2000).
7. Takeda, S. *et al.* Leptin regulates bone formation via the sympathetic nervous system. *Cell* **111**, 305–317 (2002).
8. Hanada, R. *et al.* Neuromedin U has a novel anorexigenic effect independent of the leptin signaling pathway. *Nat. Med.* **10**, 1067–1073 (2004).
9. Brighton, P.J., Szekeres, P.G. & Willars, G.B. Neuromedin U and its receptors: structure, function, and physiological roles. *Pharmacol. Rev.* **56**, 231–248 (2004).
10. Fang, L., Zhang, M., Li, C., Dong, S. & Hu, Y. Chemical genetic analysis reveals the effects of NMU2R on the expression of peptide hormones. *Neurosci. Lett.* **404**, 148–153 (2006).
11. Riggs, B.L., Khosla, S. & Melton, L.J. 3rd. A unitary model for involutional osteoporosis: estrogen deficiency causes both type I and type II osteoporosis in postmenopausal women and contributes to bone loss in aging men. *J. Bone Miner. Res.* **13**, 763–773 (1998).
12. Karsenty, G. & Wagner, E.F. Reaching a genetic and molecular understanding of skeletal development. *Dev. Cell* **2**, 389–406 (2002).
13. Harada, S. & Rodan, G.A. Control of osteoblast function and regulation of bone mass. *Nature* **423**, 349–355 (2003).
14. Idris, A.I. *et al.* Regulation of bone mass, bone loss and osteoclast activity by cannabinoid receptors. *Nat. Med.* **11**, 774–779 (2005).
15. Abe, E. *et al.* TSH is a negative regulator of skeletal remodeling. *Cell* **115**, 151–162 (2003).
16. Elefteriou, F. *et al.* Leptin regulation of bone resorption by the sympathetic nervous system and CART. *Nature* **434**, 514–520 (2005).
17. Fu, L., Patel, M.S., Bradley, A., Wagner, E.F. & Karsenty, G. The molecular clock mediates leptin-regulated bone formation. *Cell* **122**, 803–815 (2005).
18. Howard, A.D. *et al.* Identification of receptors for neuromedin U and its role in feeding. *Nature* **406**, 70–74 (2000).
19. Wren, A.M. *et al.* Hypothalamic actions of neuromedin U. *Endocrinology* **143**, 4227–4234 (2002).
20. Parfitt, A.M. The physiological and clinical significance of bone histomorphometric data. in *Bone Histomorphometry* (ed. Recker, R.R.) 143–223 (CRC Press, Boca Raton, FL, 1983).
21. Chu, C. *et al.* Cardiovascular actions of central neuromedin U in conscious rats. *Regul. Pept.* **105**, 29–34 (2002).
22. Ahn, J.D., Dubern, B., Lubrano-Berthelier, C., Clement, K. & Karsenty, G. Cart overexpression is the only identifiable cause of high bone mass in melanocortin 4 receptor deficiency. *Endocrinology* **147**, 3196–3202 (2006).
23. Kalinova, J., Triska, J. & Vrchotova, N. Distribution of vitamin E, squalene, epicatechin, and rutin in common buckwheat plants (*Fagopyrum esculentum* Moench). *J. Agric. Food Chem.* **54**, 5330–5335 (2006).
24. Zeng, H. *et al.* Neuromedin U receptor 2–deficient mice display differential responses in sensory perception, stress, and feeding. *Mol. Cell. Biol.* **26**, 9352–9363 (2006).
25. Elias, C.F. *et al.* Leptin differentially regulates NPY and POMC neurons projecting to the lateral hypothalamic area. *Neuron* **23**, 775–786 (1999).
26. Graham, E.S. *et al.* Neuromedin U and Neuromedin U receptor-2 expression in the mouse and rat hypothalamus: effects of nutritional status. *J. Neurochem.* **87**, 1165–1173 (2003).
27. Paxinos, G. & Franklin, K. *The Mouse Brain in Stereotaxic Coordinates* 2nd edn. (Academic Press, San Diego, 2001).

Ghrelin differentially modulates glucose-induced insulin secretion according to feeding status in sheep

Hideyuki Takahashi, Yohei Kurose, Muneyuki Sakaida, Yoshihiro Suzuki, Shigeki Kobayashi, Toshihisa Sugino[1], Masayasu Kojima[2], Kenji Kangawa[2], Yoshihisa Hasegawa and **Yoshiaki Terashima**

School of Veterinary Medicine and Animal Science, Kitasato University, Towada-shi, Aomori 034-8628, Japan

[1]Graduate School of Biosphere Science, Hiroshima University, Higashi-Hiroshima-shi, Hiroshima 739-8528, Japan

[2]National Cardiovascular Center Research Institute, Osaka 565-8565, Japan

(Correspondence should be addressed to Y Kurose; Email: kurose@vmas.kitasato-u.ac.jp)

(M Kojima is currently at the School of Veterinary Medicine and Animal Science, Kitasato University, Towada-Shi, Aamori 034-8628, Japan)

Abstract

The present study was conducted to investigate roles of ghrelin in glucose-induced insulin secretion in fasting- and meal-fed state in sheep. Castrated Suffolk rams were fed a maintenance diet of alfalfa hay cubes once a day. Hyperglycemic clamp (HGC) was carried out to examine glucose-induced insulin response from 48 to 53 h (fasting state) and from 3 to 8 h (meal-fed state) after feeding in Experiment 1 and 2 respectively. Total dose of 70 nmol/kg body weight of D-Lys3-GHRP6, a GH secretagogue receptor 1a (GHS-R1a) antagonist, was intravenously administered at 0, 60, and 120 min after the commencement of HGC. In the fasting state, the ghrelin antagonist significantly ($P<0·01$) enhanced glucose-induced insulin secretion. In the meal-fed state, i.v. administration of synthetic ovine ghrelin (0·04 μg/kg body weight per min during HGC) significantly ($P<0·05$) enhanced glucose-induced insulin secretion. D-Lys3-GHRP6 treatment suppressed ghrelin-induced enhancement of the insulin secretion. In conclusion, ghrelin has an inhibitory and stimulatory role in glucose-induced insulin secretion via GHS-R1a in fasting- and meal-fed state respectively.

Journal of Endocrinology (2007) **194**, 621–625

Introduction

Ghrelin is a novel peptide that acts on the growth hormone secretagogue receptor (GHS-R) in the pituitary and hypothalamus to stimulate GH secretion (Kojima *et al.* 1999, Takaya *et al.* 2000). In some species, there is evidence that ghrelin also stimulates food intake and reduces energy expenditure (Tschop *et al.* 2000, Nakazato *et al.* 2001, Wren *et al.* 2001).

Apart from these actions in the brain, ghrelin has been reported to have a dual role in the regulation of pancreatic insulin secretion. Some studies in rats show that ghrelin stimulates insulin secretion *in vivo* (Lee *et al.* 2002) and *in vitro* (Date *et al.* 2002, Adeghate & Ponery 2002). Others show that ghrelin inhibits insulin secretion from rat pancreatic islets in a dose- and glucose-dependent manner (Colombo *et al.* 2003) and from mouse islets in the presence of glucose (Reimer *et al.* 2003). GHS-R antagonist and immunoneutralization of endogenous ghrelin enhance glucose-induced insulin release from perfused rat pancreas (Dezaki *et al.* 2006). In humans, ghrelin has been shown to cause hyperglycemia by reducing insulin secretion (Broglio *et al.* 2001). These discrepancies among the effects of ghrelin on insulin secretion have not been examined.

On the other hand, blood ghrelin levels are affected by nutritional states. Plasma ghrelin levels are increased after fasting and reduced after feeding in humans (Ariyasu *et al.* 2001, Cummings *et al.* 2001, Shiiya *et al.* 2002). Lee *et al.* (2002) showed that a high-fat diet decreases plasma ghrelin levels, whereas a low-protein diet increases plasma ghrelin levels in rats. Therefore, ghrelin secretion may be enhanced under negative energy balance but inhibited under positive energy balance.

Overall, it appears that ghrelin may play an important role in glucose metabolism, through modulation of insulin secretion, but this could be dependent on whether the organisms are in negative or positive energy balance. We observed that plasma levels of ghrelin were inversely related with those of insulin around feeding in sheep (unpublished data). Furthermore, we have demonstrated that ghrelin infusion stimulates glucose-induced insulin secretion in meal-fed sheep (Takahashi *et al.* 2006). These observations led us to hypothesize that ghrelin regulates insulin secretion dependent on energy balance. In the present study, we have explored this hypothesis by examining the involvement of GHS-R1a in glucose-induced insulin secretion in fasting- and meal-fed sheep.

DOI: 10.1677/JOE-07-0206
0022-0795/07/0194–621 Online version via http://www.endocrinology-journals.org

Materials and Methods

Experimental animals and treatments

Twenty two-year-old neonatally castrated Suffolk rams of 51·4±0·3 kg were placed in metabolism cages and held at 20 °C ambient temperature under a 12 h light:12 h darkness cycle (0730–1930 h light:1930–0730 h darkness). The animals were fed a maintenance diet of alfalfa hay cubes at 0900 h each day for 10 days prior to the experimental period, with free access to water. Bilateral jugular venous cannulas were inserted one day prior to the experimentation and closed with two-way taps and filled with heparinized (40 U/ml) normal saline for infusion and blood sampling. The animals were divided into two groups ($n=4$ per group) in Experiment 1 and into three groups ($n=4$ per group) in Experiment 2.

In Experiment 1, hyperglycemic clamp (HGC; see below) was conducted in both groups from 48 to 53 h after the last feeding (fasting state), when plasma ghrelin levels reached plateau (Sugino *et al.* 2002). Ghrelin antagonist-treated group received a total dose of 70 nmol/kg body weight D-Lys3-GHRP-6 (Sigma) in normal saline via the right jugular cannula every 60 min from 0 to 120 min after the commencement of a glucose infusion via the contralateral cannula. The dose of D-Lys3-GHRP-6 was determined according to several reports (Fujino *et al.* 2003, Dezaki *et al.* 2004, Dong *et al.* 2006). The control group received saline vehicle alone. In order to determine physiological effects of ghrelin as far as possible, we avoided administering ghrelin to the fasting animals in which plasma ghrelin levels had reached plateau (2·0 ng/ml).

In Experiment 2, HGC was conducted in all groups from 3 to 8 h after feeding (meal-fed state) when plasma ghrelin levels were nadir (Sugino *et al.* 2002). Concomitantly, two ghrelin-treated groups received synthetic ovine ghrelin (Peptide Institute Inc., Osaka, Japan) in saline (0·9% NaCl, 0·1% sheep serum albumin) at a rate of 0·04 μg/kg body weight per min through the left jugular cannula. The control group received saline vehicle alone. The ghrelin plus antagonist-treated group received a total dose of 70 nmol/kg body weight D-Lys3-GHRP-6 in normal saline (or saline vehicle alone) via the right jugular cannula every 60 min from 0 to 120 min after the commencement of a glucose infusion via the contralateral cannula. In order to determine physiological effects of ghrelin as far as possible, we avoided administering the antagonist alone to the fed animals in which plasma ghrelin levels had reached nadir (0·5 ng/ml).

Blood samples were collected through the right cannula, immediately placed into a heparinized tube with aprotinin (1000 KIU/ml of blood) and centrifuged for 10 min at 4 °C. Harvested plasma was stored at −80 °C until assay.

Hyperglycemic clamp

The HGC technique was used to determine insulin responsiveness to glucose. Glucose solution was prepared at 20% (wt/vol). Basal glucose concentrations were determined three times at 10-min interval before glucose infusion. In the HGC, blood glucose levels were raised to the desired hyperglycemia (100 mg/100 ml higher than the basal blood glucose) and were maintained at that plateau by infusing the glucose solution via the right cannula with a peristaltic pump (Mode AC-2120, Atto Co. Ltd, Tokyo, Japan). Blood glucose levels were measured with a glucose analyzer (GLU-1, TOA Electronics Ltd, Tokyo, Japan) at 5-min intervals throughout the experiment, and glucose infusion rate was empirically determined.

Time-resolved fluoro-immunoassay of plasma ghrelin, insulin, and GH

Ghrelin An assay for bioactive ghrelin was done as described previously (Sugino *et al.* 2002). The ghrelin concentration was measured by competitive solid-phase immunoassay using Europium (Eu)-labeled synthetic rat ghrelin and polystyrene microtiter strips (Nalge Nunc Int., Tokyo, Japan) coated with anti-rabbit γ-globulin. Intra- and inter-assay coefficients of variation were 6·9 and 5·5% respectively. Least detectable dose and IC50 in this assay system were 0·025 and 0·831 ng/ml respectively.

Insulin Insulin assay was done as described previously (Takahashi *et al.* 2006). The insulin concentration was measured by competitive solid-phase immunoassay using Europium (Eu)-labeled synthetic bovine insulin and polystyrene microtiter strips (Nalge Nunc Int.) coated with anti-guinea pig γ-globulin. The anti-human insulin was kindly supplied by Dr. K. Wakabayashi (Biosignal Research Center, Institute for Molecular and Cellular Regulation, Gunma University). Intra- and inter-assay coefficients of variation were 3·2 and 3·1% respectively. Least detectable dose and IC50 in this assay system were 0·016 and 1·073 ng/ml respectively.

GH GH assay was done as described previously (Sugino *et al.* 2002). The GH concentration was measured by competitive solid-phase immunoassay using Europium (Eu)-labeled synthetic ovine GH and polystyrene microtiter strips (Nalge Nunc Int.) coated with anti-rabbit γ-globulin. Intra- and inter-assay coefficients of variation were 4·1 and 9·3% respectively. Least detectable dose and IC50 in this assay system were 0·158 and 8·738 ng/ml respectively.

Statistical analysis

The values of plasma ghrelin, insulin and GH concentrations, and glucose infusion rates were expressed as means±S.E.M. Repeated measures of two-way ANOVA was used to evaluate statistical significance of treatment effects on each parameter over time. Statistical comparisons for glucose, ghrelin, GH and insulin among the treatments at each time point was evaluated using the *post hoc* Fisher's test.